Agricultural and Forest Meteorology 198–199 (2014) 181–191

Contents lists available at ScienceDirect

Agricultural and Forest Meteorology

journal homepage: www.elsevier.com/locate/agrformet

Simultaneous measurements of above and below canopy ozone fluxes help partitioning ozone deposition between its various sinks in a Mediterranean Oak Forest

S. Fares[a,*], F. Savi[a,b], J. Muller[c], G. Matteucci[d,e], E. Paoletti[f]

[a] Consiglio per la ricerca e la sperimentazione in agricoltura—Research Center for the Soil-Plant System, Rome, Italy
[b] Department for Innovation in Biological, Agro-Food and Forest Systems (DIBAF), University of Tuscia, via S. Camillo de Lellis, 01100 Viterbo, Italy
[c] School of Earth, Atmospheric and Environmental Sciences, University of Manchester, Manchester, United Kingdom
[d] National Research Council of Italy, Institute of Agro-environmental and Forest Biology, Rome, Italy
[e] Institute for Agriculture and Forestry Systems in the Mediterranean, Rome, Italy
[f] National Research Council, Institute for Sustainable Plant Protection, Firenze, Italy

ARTICLE INFO

Article history:
Received 12 June 2014
Received in revised form 22 August 2014
Accepted 27 August 2014

Keywords:
Ozone fluxes
Eddy covariance measurements
Non-stomatal sink
Resistance modelling
Holm Oak Forest
Quercus ilex

ABSTRACT

Castelporziano Estate is a coastal forest 25 km from downtown Rome. It is an ideal site to study interactions between Mediterranean forest ecosystems and a polluted atmosphere. Two eddy covariance systems were used to simultaneously measure water vapour and ozone fluxes above and below a canopy of Holm Oak (*Quercus ilex*). Additional measurements of environmental parameters allowed to calculate stomatal ozone fluxes in order to parameterize atmospheric models and new algorithms for discriminating ozone deposition into its three more significant sinks: soil, stomata, and cuticles. Results showed that stomata explained almost the totality of ozone fluxes during the winter season, and <60% during the warm seasons under condition of drought stress. Soils removed up to 30% of ozone, suggesting the importance of this sink in this forest ecosystem. This study spanning all seasons over a 2-year period advanced our understanding about the contribution of a representative Mediterranean Oak forest to biosphere–atmosphere exchange.

1. Introduction

Tropospheric ozone is a secondary photochemical pollutant largely produced in the vicinity of urban areas, where precursor species such as nitrogen oxides (NO_x) and volatile organic compounds (VOC) are emitted (Monks et al., 2009). Atmospheric concentrations of ozone in northern mid-latitudes increased substantially in the past few decades (Vingarzan, 2004), with concentrations in the Mediterranean Basin being even more elevated than in Northern and Western Europe (Millan et al., 2000; Kalabokas and Repapis, 2004; Paoletti, 2006).

Forest ecosystems have the capacity to remove ozone through both stomatal and non-stomatal mechanisms (Kurpius and Goldstein, 2003; Fares et al., 2010a,b, 2012, 2013b). Environmental variables such as light, temperature and water availability in the soil-plant-atmosphere system play a major role in regulating the stomatal aperture, and hence ozone removal. Recent studies highlighted a predominant role of drought as main limiting factor in the regulation of gas exchange in Mediterranean Oak ecosystems (Vargas et al., 2013). Therefore, stomatal ozone sinks are highly variable during the year, especially in the Mediterranean area, which is characterized by a strong climate variability.

Ozone is considered a major concern for forest health (Paoletti et al., 2010; Serengil et al., 2011). Exposure to elevated ozone concentrations produces biochemical and physiological changes in plants when ozone is taken up through stomata, with inhibition of carbon assimilation by photosynthesis (Wittig et al., 2009; Fares et al., 2013a). Therefore, understanding ozone deposition pathways is a key focus of the international science community involved in risk assessment policy (UN/ECE Convention on long-range transport of air pollution, LRTAP; see http://www.unece.org/env/lrtap).

Non-stomatal ozone sinks can represent the major component of total ozone deposition to forest ecosystems (Fowler et al., 2009). These sinks consist of ozone removal on plant surfaces and in soils. They may also include chemical sinks in the atmosphere and in soil, represented by nitric oxide (NO) and reactive VOC (Nemitz et al., 2000; Kurpius and Goldstein, 2003; Farmer and Cohen, 2008). The capacity to measure and model these ozone sinks is important to

* Corresponding author. Tel.: +39 06 7005413 127.
E-mail address: silvano.fares@entecra.it (S. Fares).

http://dx.doi.org/10.1016/j.agrformet.2014.08.014
0168-1923/

quantify the role of peri-urban forests in phytoremediation, as an additional ecosystem service provided to the community (Groot et al., 2002; Escobedo and Nowak, 2009).

Considering the importance of ozone effects on Mediterranean vegetation and the potential of peri-urban forests in mitigating ozone concentrations, we set up an experimental site in a typical Mediterranean forest dominated by Holm Oak. We measured ozone and water vapour fluxes continuously for two years using the eddy covariance technique above the canopy to answer a first research question: what is the stomatal contribution to ozone deposition during the main seasons? A second eddy covariance system was equipped below the canopy, in order to estimate the soil contribution to ozone deposition fluxes and quantify water evaporation. Experimental data were used to test empirical models and predict ozone deposition to cuticles and soil. The models were then used to address a second research question: what is the contribution of the main non-stomatal sinks to the total ozone flux budget across the seasons?

2. Material and methods

2.1. Site description

The Presidential Estate of Castelporziano covers an area of about 6000 ha, is located 25 km SW from the Center of Rome, Italy, and is part of the Italian network for Long Term Ecological Research. This Thermo-Mediterranean region is characterized by stress aridity in summer, and moderate cold stress in winter. The experimental site inside the Estate is named "Grotta di Piastra" (41.42N, 12.21E), located at 13 m a.s.l. and 1.5 km from the seashore of the Thyrrenian sea. Thirty-minute averages of photosynthetically active radiation (PAR), air temperature and vapour pressure deficit (VPD) for 2013 are shown in Fig. 1. As the growing season is all-year round with peaks in carbon assimilation in spring and early fall and decreased levels in summer due to temperature stress, data were averaged for each season. Mean annual precipitation was 805 ± 256 mm, as averaged over the years 2007–2011. Wind circulation is mostly determined by a local sea-land breeze wind regime, with moderate to strong S–SW winds blowing in the morning, and light N–NE winds in the afternoon. The soil has a sandy texture and low water-holding capacity, which exacerbates drought. More details on soil properties and site characteristics are provided in Fares et al. (2009, 2013b).

The tower footprint, estimated according to Hsieh et al. (2000), was dominated by *Quercus ilex*. Within the footprint area, total Leaf Area Index (LAI) was 3.69 $m^2{}_{leaf}\, m^{-2}{}_{ground}$, measured using a LAI-2000 instrument (LI-COR, Licoln, NE, USA) with an average canopy height of 14.9 m.

2.2. Meteorological parameters

Meteorological sensors were installed at canopy level (14 m) onto a 19-m high tower. Relative humidity, air temperature, net solar radiation, precipitation and leaf wetness were measured every minute and averaged at 30-min intervals with a Davis vantage pro meteorological station (Davis Instruments Corp. CA, USA). A sonic anemometer (Gill Windmaster) was used to instantaneously measure wind speed and direction. Photosynthetic photon flux density was measured with a LI-190 Quantum sensor (LI-COR, Licoln, NE, USA), and signal recorded using a data logger (CR3000, Campbell Scientific, Shepshed, UK). Leaf temperature of 3 sun leaves and 3 shade leaves was recorded with custom-made thermocouples and recorded using a data logger (CR23x, Campbell Scientific, Shepshed, UK). Soil moisture and temperature were measured at 10, 50, and 100 cm depths using capacitive relative humidity sensors (CS 650, Campbell Scientific).

Ozone concentrations were measured using a UV photometric ozone analyzer (49i, Thermo Scientific), with a precision of 0.5 ppb. Measurement heights were 19.7 m (above canopy), 14.9 m (canopy level) and 2.4 m (soil level). Air was sampled using separate sampling lines (20-m long Teflon tubes, with 4-mm inner diameter) through which air flowed continuously to avoid any memory or surface effects. To avoid contamination and flow problems, Teflon filters (PFA holder, PTFE membrane, 2 μm pore size) were installed at the sampling inlets and replaced every two weeks. A custom-made valve system sampled ozone sequentially for 6 min at each measuring height. Data collection and sampling system control were performed using a data logger (CR3000, Campbell Scientific, Shepshed, UK).

2.3. Above-canopy eddy covariance measurements

Flux measurements at canopy level started in January 2012 and ended in December 2013. Wind velocity and sonic virtual temperature fluctuations were measured at 10 Hz with a three-dimensional sonic anemometer (Gill Windmaster, Gill Instruments, Lymington, UK) mounted on a horizontal beam next to the inlet of the sampling line. Air was sampled continuously at 19.7 m height near the sonic anemometer. The trace gas analytical equipment (for H_2O and O_3) was housed in an air-conditioned cabin at the bottom of the measurement tower. Ozone measurements were made by chemiluminescence using coumarin dye with a custom-made instrument developed by the National Oceanic and Atmospheric Administration (NOAA, Silver Spring, MD, Bauer et al., 2000). The chemiluminescence signal was calibrated against 30-min average ozone concentrations from the UV ozone monitor. Water vapour concentrations were measured using a closed path infrared gas analyzer (LI-7200, Lincoln, NE, USA). The raw analogue data for all gases were recorded at 10 Hz, and logged with the data by the sonic anemometer by a LI-COR datalogger (LI-7550, Lincoln, NE, USA). Ozone and water vapour concentrations measured at 19.7 m height were filtered by removing values exceeding six standard deviations in a one-minute window. Water concentrations were corrected for a spectroscopic effect (Detto and Katul, 2007) due to fluctuations in temperature and water vapour (WPL theory, Webb et al., 1980), using temperature and pressure values measured inside the instrument cell. Corrected concentrations were correlated with the vertical wind velocity over 30-min intervals according to the eddy covariance technique extensively described in Aubinet et al. (2012). The time lag for sampling and instrument response was determined by maximizing the covariance between vertical wind velocity and scalar fluctuation. Errors due to sensor separation and damping of high frequency eddies were corrected using spectral analysis techniques as outlined by Rissmann and Tetzlaff (1994). The wind data were rotated according to the planar fit method (Wilczak et al., 2001). A stationary test was performed according to the method described by Foken and Wichura (1996). When the stationary test result was above 30%, data were discarded. This led to a data removal of 11% and 15% for ozone and water fluxes, respectively. Friction velocity was used to identify low turbulence periods. Thresholds were evaluated according to the 99% threshold criterion on nighttime data (Papale et al., 2006), and the dataset was filtered according to the highest threshold found. Eddy covariance data quality was also evaluated through spectral analysis, performed by using averaged binned cospectra of scalars and vertical wind velocity. Cospectra were calculated only for daytime periods (solar radiation >100 W m^{-2}) under unstable conditions ($(z_c - d)/L < 0$, where z_c is the canopy height, d the displacement height and L is the Monin–Obukhov length), high turbulence and homogeneous boundary layer ($\overline{v'w'}/u'\bar{w}' < 0.25$, where $\overline{v'w'}$ and $u'\bar{w}'$ are lateral

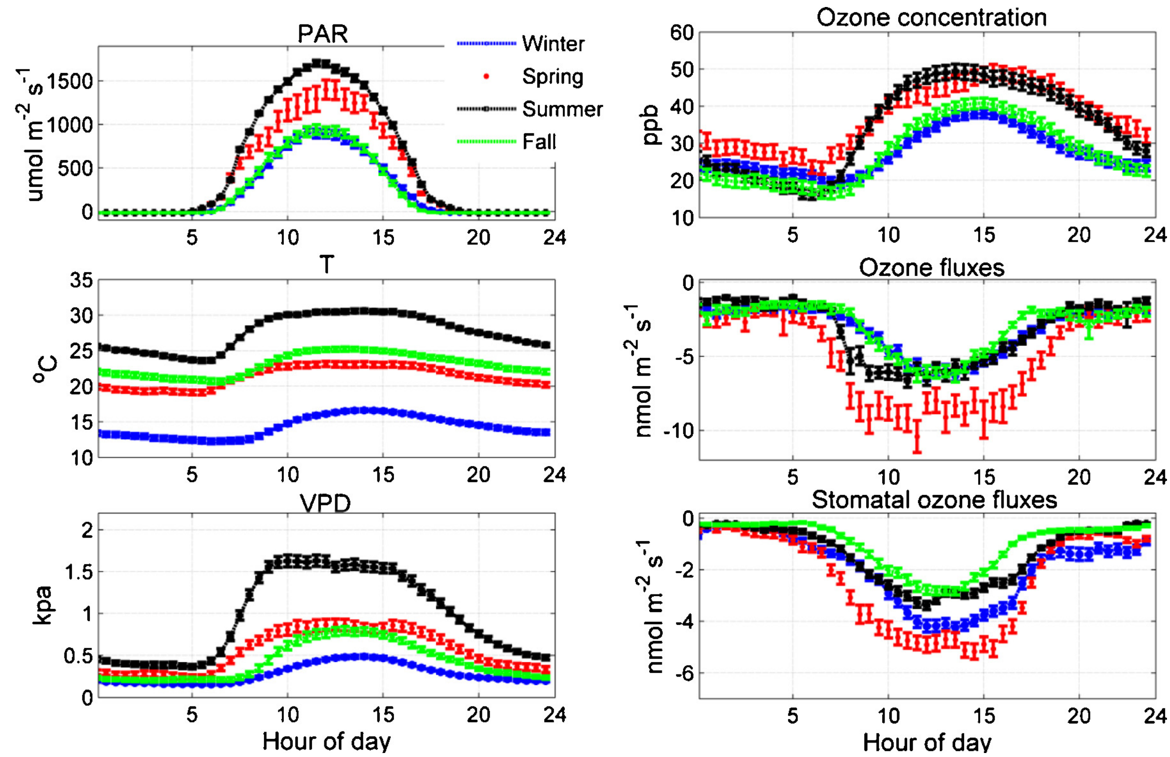

Fig. 1. Thirty-minute ensemble average diurnal cycles (±standard deviation) of photosynthetically active radiation (PAR), air temperature, vapour pressure deficit (VPD), ozone concentration, total and stomatal ozone fluxes for the each season of the year 2013.

and longitudinal momentum fluxes, respectively, Smeets et al., 2009). Averaged cospectra (Fig. 2) showed fall-off slopes for ozone and water close to a −7/3 trend similar to the sensible heat flux. Compared with the sensible heat cospectrum, above-canopy measurement showed slightly higher frequency attenuation in both water and ozone cospectra.

Stomatal resistance to water vapour (R_{sto}) was calculated from the eddy covariance measured evapotranspiration using the evaporative/resistance method (Monteith and Unsworth, 1990; Turnipseed et al., 2009; Fares et al., 2012, 2013b):

$$R_{sto} = \frac{cp \times \rho \times \mathrm{VPD}}{\lambda \times \gamma \times E_L} - (R_a + R_b) \quad (1)$$

where λ is the latent heat of vaporization in air (J kg^{-1}), γ is the psychrometric constant (0.065 kPa K^{-1}), E_L is the transpiration rate (kg H_2O m^{-2} s^{-1}) after subtracting the evaporative contribution from soil calculated with below-canopy eddy covariance measurements (details provided below), cp is the specific heat of air (J kg^{-1} K^{-1}), ρ (kg m^{-3}) is the density of dry air, VPD is the vapour pressure deficit at leaf level (kPa), R_a and R_b (s m^{-1}) are the aerodynamic and laminar sublayer resistances. Stomatal conductance to ozone (G_{O_3}) was calculated as the inverse of R_{sto} corrected for the difference in diffusivity between ozone and water vapour (Massman, 1998). Stomatal ozone flux (F_{O_3}) was calculated by multiplying G_{O_3} by ozone concentration assuming that intercellular concentration of ozone is zero (Laisk et al., 1989). This

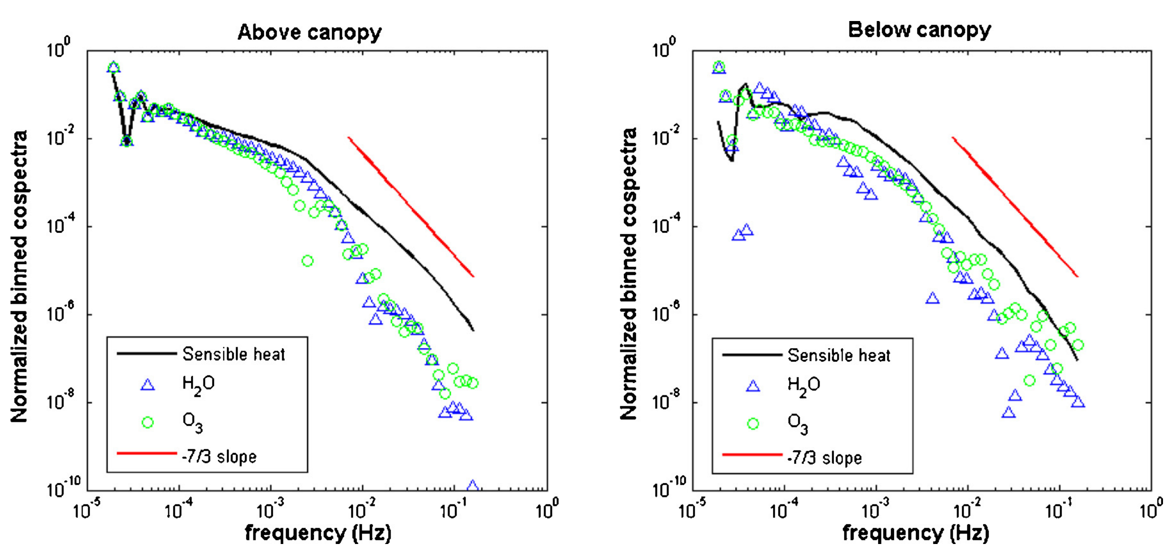

Fig. 2. Normalized cospectral density of sensible heat, ozone and water above and below the canopy.

assumption has been rejected in case of exposure to concentration of ozone above 100 ppb and high level of stomatal aperture (Fares et al., 2010b); however our field site was characterized by <80 ppb ozone concentrations and by a limited stomatal conductance, therefore the possibility of ozone accumulation inside the leaves was unlikely.

In order to minimize the effect of soil and surface evaporation on total evapotranspiration (and therefore not to overestimate G_{O_3}), measurements of the three days following precipitation and episodes of leaf wetness were discarded.

Total ozone fluxes were divided by ozone concentration to obtain deposition velocity (Vd_{O_3}). Canopy conductance to ozone (G_c) was calculated from Vd_{O_3} taking into account atmospheric resistances as reported by Fares et al. (2012, 2013a).

In this work, fluxes are expressed per unit of ground area (m^2); positive fluxes indicate upward mass and energy exchanges from the ecosystem to the atmosphere, and negative fluxes indicate transfer from the atmosphere into the ecosystem.

2.4. Below-canopy eddy covariance measurements

Eddy covariance fluxes of water vapour above the forest floor were measured from 15 July to 26 November 2013 (Julian days 196–330) using a closed path infrared gas analyzer (LI-7000, Lincoln, NE, USA), installed in the air-conditioned cabin at the bottom of the tower. Ozone fluxes were measured from 27 June to 23 August 2013 (Julian days 178–235) using a dry chemiluminescence Rapid Ozone Flux Instrument (ROFI Mk2, Muller et al., 2010). All trace gases were logged at 10 Hz along with the turbulence measurements made by a sonic anemometer (RM Young 81000, RM Young Company, Michigan, USA), mounted at 2.4 m above the forest floor, less than 10 m away from the flux tower. The ROFI instrument was mounted on the mast, sampling just below the sonic anemometer. The inlet for H_2O fluxes was co-located, and the sampling flow through the 20-m long Teflon (PFA) tubing (4-mm internal diameter) was constant at 12 slpm to maintain turbulent flow conditions. Ozone concentrations measured at 2.4 m above soil were used for absolute rescaling of the relative ozone signal from the fast ozone analyzer. Chemiluminescence reactant discs (Bagus Consulting, Speyer, Germany) were changed weekly. Half-hourly turbulent fluxes were calculated and corrected using the same procedure for above-canopy measurements, as described above. Data which did not pass the stationary test were 62% and 52% for ozone and water fluxes, respectively. 65% of the data were below the u^* threshold and were discarded. Averaged cospectra showed fall-off slopes for ozone and water close to a −7/3 trend similarly to the sensible heat flux (Fig. 2). Only sparse vegetation dominated by *Pistacia lentiscus* was present between this second eddy covariance system and the ground level, thus this second measuring station represents the contribution by soil and leaf litter to the ozone and water vapour fluxes.

2.5. Modelling ozone and water vapour fluxes at soil level and ozone cuticular deposition

Based on the measured fluxes, we developed an empirical model to calculate water vapour and ozone fluxes. The model was based on step-wise regression according to the least squares method of the general linear model. Several case studies are reported in Table 1. The equation for water fluxes at ground level ($H_2O\text{flux}_{\text{soil}}$, mmol m^{-2} s^{-1}) used four significant predictors: soil moisture (SWC10, %) and soil temperature (Ts10, °C) at 10 cm depth, friction velocity (u^*, m s^{-1}) and water fluxes above the canopy (H_2Oflux, mmol m^{-2} s^{-1}):

$$H_2O\text{flux}_{\text{soil}} = b_0 + b_1\text{SWC10} + b_2\text{Ts10} + b_3u* + b_4H_2O\text{flux} \quad (2)$$

The equation for ozone fluxes at ground level ($O_3\text{flux}_{\text{soil}}$, nmol m^{-2} s^{-1}) included three predictor variables measured above the canopy level: ozone concentration ([O_3], ppb), friction velocity (u^*, m s^{-1}) and air temperature (T_a, °C):

$$O_3\text{flux}_{\text{soil}} = b_0 + b_1[O_3] + b_2u* + b_3T_a \quad (3)$$

Data averaged for 30-min time resolution were used in the model. The models were built with randomly selected 70% of the dataset and then cross-validated with the remaining 30% of the data. The relation between measured and predicted values was tested by linear regression analysis to check the goodness of the models.

A previously used atmospheric model was also used to calculate ozone deposition to soil. This includes calculation of below-canopy resistances estimated as the sum of in-canopy aerodynamic resistance (R_{ac}, s m^{-1}) and ground resistance (R_g, s m^{-1}), calculated according to Erisman et al. (1994), Zhang et al. (2002), Meszaros et al. (2009) and Fares et al. (2012):

$$R_{\text{ac}} = \frac{14 \times \text{LAI} \times z_c}{u*} \quad (4)$$

$$R_g = R_{g1} + R_{g2} \cdot \frac{\text{SWC10}}{\text{SWC}_{\text{fc}}} \quad (5)$$

where z_c is the canopy height (m), R_{g1} and R_{g2} are constant resistances (s m^{-1}) which we calculated iteratively by comparing modelled and measured values, SWC_{fc} is the volumetric soil water content at field capacity (28%) calculated as the maximum value of SWC10 (%) after precipitation events.

The inverse of these resistances were multiplied by the ozone concentration measured at soil level (2.4 m) to estimate ozone flux at soil level.

Cuticular resistance (R_{cut}, s m^{-1}) was calculated according to the deposition model by Zhang et al. (2002) for both wet and dry canopy:

$$R_{\text{cut(dry)}} = \frac{R_{\text{cut(dry)}_0}}{e^{0.03RH} \times \text{LAI}^{1/4} \times u*} \quad (6)$$

$$R_{\text{cut(wet)}} = \frac{R_{cut(wet)_0}}{\text{LAI}^{1/2} \times u*} \quad (7)$$

where $R_{\text{cut(dry)}_0}$ and $R_{\text{cut(wet)}_0}$ are reference values (6000 and 400 s m^{-1}, respectively) suggested by Zhang et al. (2002) for deciduous species; RH is the relative humidity measured at canopy level (%). We assumed wet conditions when RH was more than 60% or the leaf wetness sensors placed on the canopy indicated wetness, similarly to Fares et al. (2012).

3. Results and discussion

3.1. Ozone concentrations and fluxes

Figs. 1 and 3 show the seasonal dynamics of air temperature, vapour pressure deficit, ozone concentration and fluxes during the years 2012 and 2013, and the daily trend of 30-min averages for the four seasons of year 2013, respectively. The study site was characterized by moderately cold winters and warm and dry summers. The annual mean temperatures were 16.1 ± 7.4 °C and 15.8 ± 6.8 °C for 2012 and 2013, respectively.

The highest concentrations of ozone were observed during the summer days (Figs. 1 and 3). This is consistent with the photochemical origin of ozone, which is dependent on solar radiation and temperature (Pellegrini et al., 2007). The daily dynamics of ozone concentrations showed peaks between 02:00 and 03:00 PM, similarly to previous observations in Castelporziano (Fares et al., 2009, 2013b) and other sites in the world (e.g. Paoletti, 2006; Fares et al., 2010b; Seok et al., 2013), suggesting that photochemically

Table 1
Results from step-wise regression analysis. For prediction of water and ozone fluxes below the canopy, 4 cases were analyzed, each one with different combination of predictors. The first case studies only use the meteorological variables. For the other case studies we introduced measured fluxes of water and ozone, with the intent to show the capacity of the model to predict water and ozone fluxes below the canopy with and without use of flux variables which require use of eddy covariance. n.a. = not available in the case study. The significant predictors which were included in the model are in bold. R^2 from linear correlation between measured data and modelled data was calculated using the 30% of the data not used to parameterize the model.

Predictors for H_2O flux below canopy	Casel		Case 2		Case 3		Case 4	
	Coeff	*P*	Coeff	*P*	Coeff	*P*	Coeff	*P*
Soil U RIO	−0.0637	0.5149	−0.2719	0.0019	−0.0807	0.2403	−0.2693	0.0047
Soil UR 50	0.1035	0.1480	n.a.	n.a.	n.a.	n.a.	n.a.	n.a.
Soil UR100	0.0642	0.4134	n.a.	n.a.	n.a.	n.a.	n.a.	n.a.
Soil T10	**0.0112**	**<0.0000**	**0.0026**	**0.0261**	−0.0017	0.175	**−0.0081**	**<0.0000**
Soil T50	0	0.8267	n.a.	n.a.	n.a.	n.a.	n.a.	n.a.
Soil T100	−0.0018	0.3075	n.a.	n.a.	n.a.	n.a.	n.a.	n.a.
*u**	**1.5651**	**<0.0000**	**0.0439**	**0.0005**	n.a.	n.a.	**1.417**	**<0.0000**
*u** Soil level	n.a.	n.a.	n.a.	n.a.	**1.2777**	**<0.0000**	**0.0118**	**<0.0000**
H_2O flux	n.a.	n.a.	**0.0428**	**<0.0000**	n.a.	n.a.	n.a.	n.a.
Tair soil level	n.a.	n.a.	n.a.	n.a.	**0.0084**	**<0.0000**	**−0.0545**	**0.0001**
Tair above canopy	n.a.	n.a.	n.a.	n.a.	n.a.	n.a.	−0.0034	0.1751
Cross-validation								
R^2	0.3161		0.4504		0.1339		0.3999	
Intercept	−0.2063		0		−0.02		−0.03	
DF	2455		2085		2557		2481	
Predictors for O_3	Casel		Case 2		Case 3		Case 4	
Flux below canopy	Coeff	*P*	Coeff	*P*	Coeff	*P*	Coeff	*P*
$[o_3]$	**−0.0431**	**<0.0000**	**0.0485**	**<0.0000**	**−0.044**	**<0.0000**	**−0.0406**	**<0.0000**
*u**	**−1.3586**	**<0.0000**	n.a.	n.a.	n.a.	n.a.	**−1.9604**	**<0.0000**
*u** Soil level	n.a.		**−21.7161**	**<0.0000**	**−15.7571**	**<0.0000**	n.a.	n.a.
Tair above canopy	−0.0215	0.4269	−0.0267	0.1997	0.0368	0.1825	0.0806	0.0118
O_3 flux	n.a.		n.a.	n.a.	0.1064	<0.0000	0.1174	<0.0000
Cross-validation								
R^2	0.6231		0.571		0.6551		0.6674	
Intercept	0.8423		2.0248		1.9668		−0.5236	
DF	406		408		283		282	

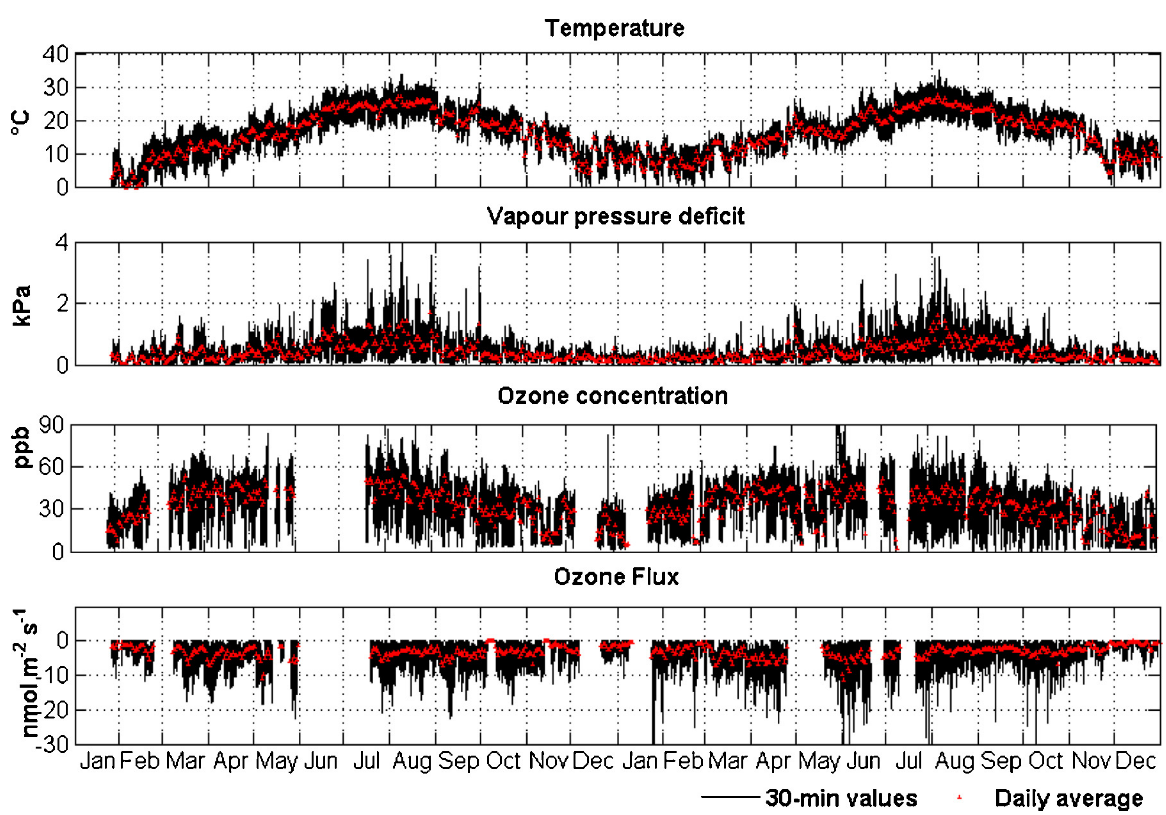

Fig. 3. Air temperature, vapour pressure deficit, ozone concentration and total ozone flux from January 2012 to December 2013. Data are shown at 30-min time resolution, daily averages are also shown.

produced ozone accumulates in the boundary layer before it is removed in the late afternoon hours.

Our field site is characterized by a typical sea-land breeze regime, with typical S–SW winds blowing during the day (from the sea) and typical N–NE winds blowing during the evening hours and night (from the land). The results suggest that meteorology may seriously affect concentrations of ozone at the site, carrying polluted air plumes from the city or from the sea. Differences were indeed observed in ozone concentration in the plumes coming from the sea and from the land during the central hours of the day (Fig. 4), suggesting that air coming from the city area is depleted in ozone especially at night due to reactions of ozone with NO and hydrocarbons emitted by vehicles and industrial activities, as previously reported by Fares et al. (2009). Under these conditions we observed ozone concentrations which normally did not exceed 60 ppb even during the warmest hours of the summer days, and ozone concentrations between 10 and 30 ppb at night, resulting from intense nighttime scavenging of ozone, including titration by NO. Air coming from the sea showed higher concentrations of ozone than air coming from the city, mainly due to slow ozone deposition on water and the capacity of the air masses above the sea to form ozone through photochemical reactions (Velchev et al., 2011). Interestingly, night concentration of ozone were significantly greater when air came from the sea especially during summer when the typical land/sea breeze regime pattern is more consistent. This suggests that newly emitted anthropogenic gases (e.g. NO emitted in the city area) could react fast with ozone thus leading to ozone-depleted air advected to our forest site, while stagnating air above the sea – which is relatively depleted of such reactive anthropogenic compounds – contains more ozone photochemically produced.

3.2. Partitioning of ozone fluxes

Fluxes were partitioned for the four seasons, based on the notion that sinks will change in response to meteorological variables and plant phenology during the year. Only ozone fluxes from 2013 were used in this analysis because evapotranspiration data were not available in the 2012 dataset. Our studies were focused on the three main ozone sinks: stomata, soil and cuticles. Other possible sinks are discussed later in the text.

3.3. Stomatal ozone fluxes

Stomatal fluxes in our site were observed in each season as a result of the long vegetative period which often lasts all the year round for Mediterranean evergreen broadleaf species like Holm Oak (Manes et al., 2007). As previously observed (Gerosa et al., 2009; Fares et al., 2010b, 2012, 2013b), total ozone fluxes peaked during the central hours of the day as a result of stomatal and non-stomatal sinks (Fig. 1). Moreover, as discussed previously (Fares et al., 2013b), a mid-day depression of fluxes due to the decreased physiological activity of plants may not be associated with limited soil moisture but rather be a result of a VPD effect on leaves (Manes et al., 1997; Mereu et al., 2009; Turnipseed et al., 2009; Fares et al., 2010b). Stomatal ozone flux peaked in spring ($-10\,\mathrm{nmol\,m^{-2}\,s^{-1}}$) when precipitation was abundant and soil water content was above 20%. Annual total precipitation was 665 mm in 2013, of which 20% fell in spring. During fall and winter, precipitation reached values of 269.4 mm and 249.1 mm, respectively.

During summer, maximum total ozone deposition fluxes were only $-6\,\mathrm{nmol\,m^{-2}\,s^{-1}}$. In the same season and site in 2004, Gerosa et al. (2009) reported fluxes up to $-16\,\mathrm{nmol\,m^{-2}\,s^{-1}}$, which remained consistently high until the fall season. However, the summer of 2004 was characterized by higher precipitation (125.4 mm vs 27.2 mm in summer 2013), in line with the 12-y average (from 1999 to 2010) of 127.0 ± 27.2 mm. Average air temperature in summer 2004 was 22 °C, whereas average air temperature in summer 2013 was higher (23.3 °C). We therefore conclude that a decrease in stomatal conductance is necessarily connected to a low water content in soil, with almost no precipitation and volumetric water content below 5% (data not shown), but it is also related to the high VPD values (Fig. 1) which are responsible for stomatal closure, as previously reported for the same type of vegetation (Manes et al., 1997).

Stomatal closure was responsible for low ozone fluxes during fall as a result of persisting conditions of drought and high temperatures (15.9 °C), but also a decrease in water table height resulting from persistent decrease in precipitation during the summer period (data not shown). Our results are consistent with recent findings that found drought stress as the main limiting condition for growth in Mediterranean Oak ecosystems (Vargas et al., 2013). Ozone fluxes during winter were low, although the mild temperatures in November (mean 13.1 °C) and at the end of the season promoted suitable conditions for vegetative growth. This may help explaining the high levels of stomatal ozone fluxes in winter, which were as high as in spring.

In order to minimize the errors associated with the water evaporation component in the canopy evapotranspiration term in Eq. (1), we directly measured soil evaporation using a second eddy covariance system below the canopy, as suggested by Wilson et al. (2001). The results were used to parameterize an empirical model of soil evaporation. A comparison of above and below canopy water fluxes shows similar peaks during the central hours of the day in response to temperature and solar radiation, but soil contribution to total evapotranspiration was still <16% (Fig. 5). Soil evaporation modelled using Eq. (2) and case study 2 (Table 1) showed a good agreement with measured values ($R^2 = 0.45$, Table 1), although an underestimation of 32% was observed comparing the daily course of modelled values vs measured values (Fig. 5). Because the eddy covariance footprint is much smaller below the canopy than above the canopy, soil evaporation is measured over a much smaller area than evapotranspiration (Wilson et al., 2001). These representativeness errors were previously found to be on the order of 10% (Wilson and Meyers, 2001). A visual inspection highlighted that the model could not predict spikes in water evaporation from soils after precipitation events and fast increases in soil temperature. However, the low contribution (and associated error) of water fluxes from soil tends to suggest that no major errors in stomatal conductance were produced. In this study, we adopted the formulation proposed in case study 2 for modelling soil evaporation. The rationale behind this decision was that R^2 reached the highest value and the predictors are potentially applicable to other Mediterranean forest ecosystems where soil moisture, temperature, u^* and water fluxes are measured above the canopy. However, we recommend the application of this algorithm only to ecosystems with characteristics of soil and vegetation similar to our field site, since the model has not been tested for other forest ecosystems.

3.4. Ozone deposition to soil

This study presents for the first time a direct quantification of ozone deposition to soil in a *Q. ilex* forest. Few eddy covariance measurements of ozone flux have been undertaken below or within forest canopies (Meyers and Baldocchi, 1993; Lamaud et al., 2002; Dorsey et al., 2004; Launiainen et al., 2013). Some studies have focussed on deposition to the forest soil only (Meyers and Baldocchi, 1993), or included above canopy and soil + understorey with the aim to partition the total ozone sink (e.g. Lamaud et al., 2002; Launiainen et al., 2013).

Ozone deposition to forest soil has been found to vary from 5 to 39% of the total deposition (Dorsey et al., 2004), when it was largest at night (39%), whereas uptake by soil and understorey

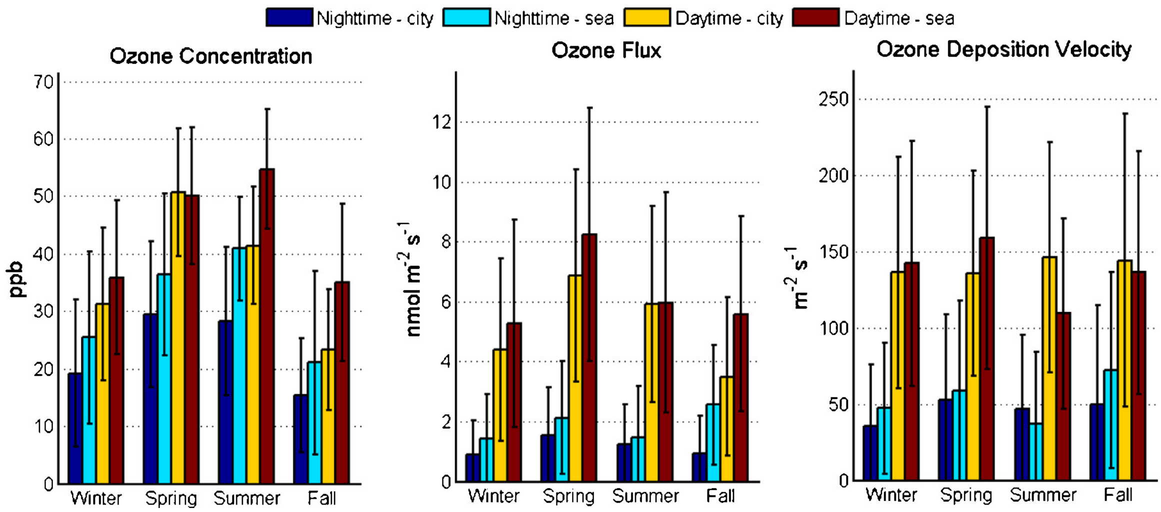

Fig. 4. Thirty-minute average (±standard deviation) of ozone concentration, ozone fluxes and ozone deposition velocity for the year 2013. For each season, data collected at 30-min time resolution were averaged for the central hours of the day (10:30 AM to 02:30 PM) and night (11:00 PM to 3 AM). Data were filtered for wind coming from the sea (SW) and wind coming from the city of Rome (NE).

was reported smallest at night (25% of total flux) by Lamaud et al. (2002). Daytime and nighttime partitioning can vary with sites, with understorey and forest floor deposition contributing up to 25–30% (nighttime) and 35–45% (daytime) to the total ozone deposition (Launiainen et al., 2013). A range of factors are likely to be responsible for this variability, such as tree density, surface wetness and possible chemical sinks (e.g. NO emitted from soil) as reported by Dorsey et al. (2004). At this particular Mediterranean forest site, surface chemical sinks by reaction with NO are not expected to be important, as discussed below.

Similar to water fluxes, below-canopy ozone deposition was modelled by means of a polynomial regression with the intent to gap-fill ozone flux to soil and compare it with above-canopy ozone flux measured for the entire year. The model was run in four case studies testing different combinations of predictors: air temperature above the canopy, u^* measured above the canopy and at the soil level, and ozone concentration (Table 1). All case studies seemed to predict well ozone fluxes at soil level ($R^2 > 0.57$). For comparison with measured fluxes, we adopted the equation resulting from the first case study (Eq. (3), $R^2 = 0.62$) due to its easy application using just two predictors: ozone concentration and u^* measured above the canopy. A good agreement between modelled and measured data was achieved (Fig. 6), mainly because the physical process of ozone deposition to soil is well represented by turbulence and ozone concentration. The dominance of u^* and hence dynamic processes in controlling the deposition to soil was also observed by Lamaud et al. (2002), particularly during nighttime and during dry surface conditions. However, the use of polynomial regression may hold only in forest sites under similar environmental and vegetation characteristics as those found in our field site. This simple empirical method may therefore not be applicable to other plant ecosystems.

In order to test a more conventional meteorological model with potential broad applications to other forest ecosystems, we tested a previously adopted empirical algorithm (Eqs. (4) and (5)). In particular, Meszaros et al. (2009) and Fares et al. (2012) adopted this model for a grassland and an orange crop, with values of R_{g1} and R_{g2} of 200 and 300 s m^{-1}, respectively. By linear correlation with measured flux data, we obtained a 30% over-prediction of fluxes using the previously reported coefficients ($R^2 = 0.19$). We

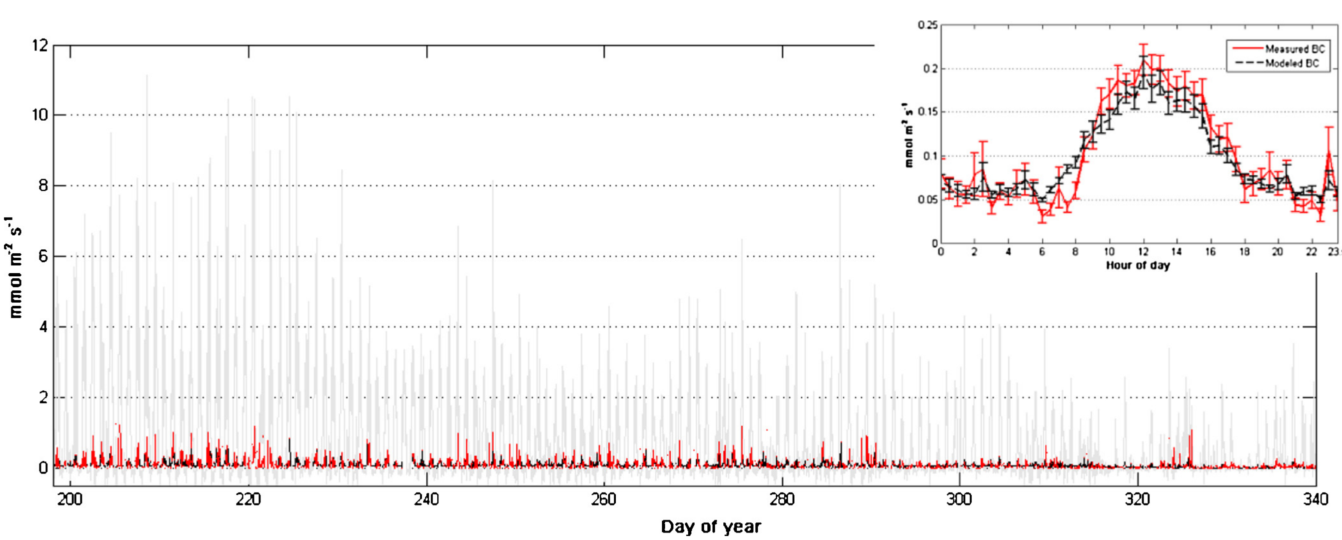

Fig. 5. Measured evapotranspiration with eddy covariance above the canopy (grey line), and soil evaporation below the canopy (BC, red line) from the Julian day 196 to the Julian day 330 of the year 2013. Diurnal cycle of soil evaporation modelled by Eq. (6) for the same time frame is also reported as 30-min ensemble average (±standard deviation). (For interpretation of the references to color in this figure legend, the reader is referred to the web version of this article.)

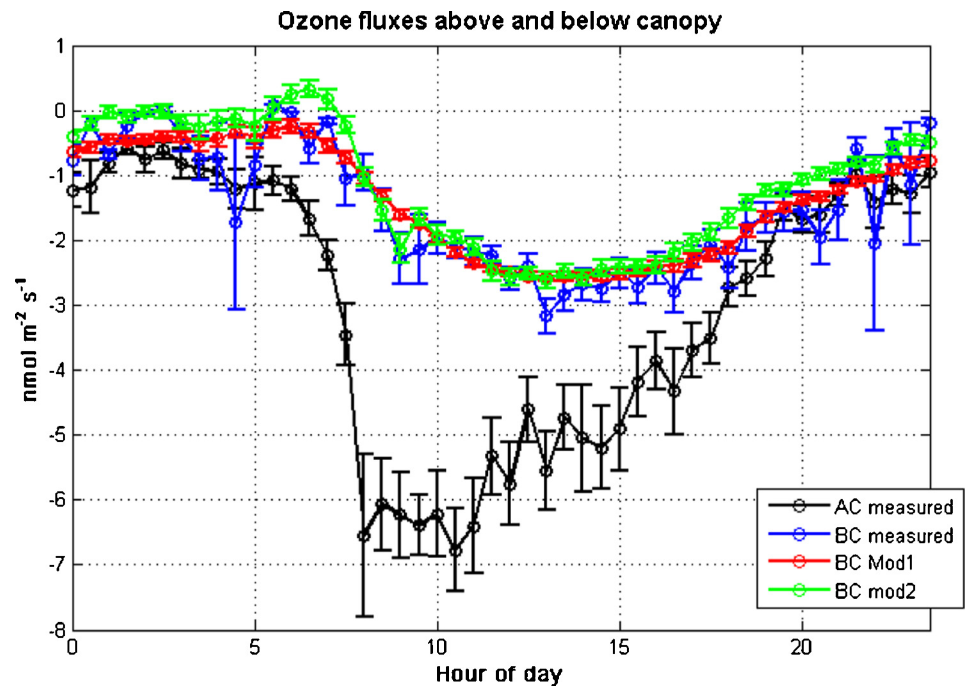

Fig. 6. Thirty-minute average (±standard deviation) of total ozone fluxes measured above the canopy (AC) (n = 2182), below the canopy (BC) (n = 2562), modelled according to Eq. (7) (mod 1) and modelled according to Eqs. (4) and (5) (mod 2). The averages were performed for the time period from the day of the year 178 to the day of the year 235, when below-canopy ozone flux measurements were performed.

therefore calculated R_{g1} and R_{g2} iteratively by comparing measured and modelled fluxes. Our best results produced values of 50 and 500 s m^{-1} for R_{g1} and R_{g2}, respectively. The new coefficients helped to reach a slope between measured and modelled fluxes closer to 1 (slope = 0.85, R^2 = 0.2) although the statistical significance was still poor due to high scattering of the variables employed in the model (SWC and R_{ac}). Results shown as 30-min averages in Fig. 6 also suggest that: (1) daytime below-canopy ozone fluxes during the period in which they were directly measured were about 2 times lower than the total above-canopy ozone fluxes; (2) night-time ozone deposition to soil was almost negligible, an indicator that when stomatal aperture is minimized other sinks may be responsible for ozone removal (about −1 nmol m^{-2} s^{-1}); (3) a good agreement was achieved between measured and modelled fluxes using both modelling approaches.

3.5. Other ozone sinks

Deposition to cuticles has been shown to be an important sink for ozone, with values spanning from 10 to 57% in a range of agricultural and forest ecosystems (Tuzet et al., 2011; Fares et al., 2012). Direct measurements by a mass-balance approach suggested that cuticular deposition of ozone is negligible when measured at leaf level (Pleijel et al., 2004; Grulke et al., 2007). In this study, cuticular deposition of ozone modelled by Eqs. (6) and (7) according to Zhang et al. (2002) showed nocturnal averages of −0.5 nmol m^{-2} s^{-1} (data not shown) and maximum values during the day of −2.5 nmol m^{-2} s^{-1}, thus representing up to 30% of total ozone fluxes (Fig. 7). The data refer to the same temporal window used in Fig. 5 i.e. the time of the year when below canopy eddy covariance measurements of water fluxes were performed (DOY 198–340). Whilst the soil fluxes were validated by measurements, cuticle deposition still remained uncertain due to the lack of experimental validation.

In this work, we focused on the three main components typically included in multi-layer models (e.g., Baldocchi, 1988), as they are likely the most representative sinks for our Mediterranean

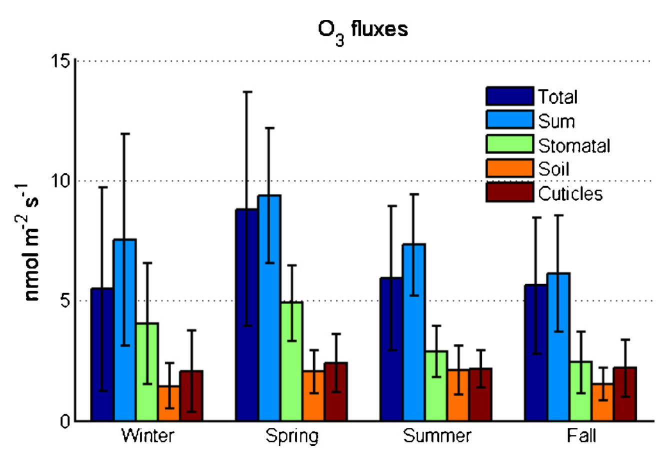

Fig. 7. Bar chart showing total, stomatal, cuticular and ground ozone fluxes. The sum of the three measured ozone sinks is also shown to highlight divergence with total ozone fluxes. For each season, data collected at 30-min time resolution were averaged for the central hours of the day (10:30 AM to 02:30 PM) (±standard deviation).

site: stomata, cuticles, and soil. However, gas-phase chemical reaction with biogenic volatile organic compounds (BVOC) have been found to explain up to 26% of total ozone fluxes for pine and crop ecosystems (Kurpius and Goldstein, 2003; Fares et al., 2010a, 2012; Oettl and Uhrner, 2011). The emission of reactive BVOC depends exponentially on air temperature, and in most cases it does not depend on stomatal conductance (Loreto and Fares, 2013). Reactive BVOC as sesquiterpenes and monoterpenes have been previously described as emitted from Mediterranean vegetation in Castelporziano (BEMA, 1997; Fares et al., 2009; Davison et al., 2009). Some sesquiterpene species react with ozone on the order of a few seconds, but they are poorly emitted by Holm Oak, which is the dominant species in our field site (Ciccioli et al., 2003; Fares et al., 2009). Monoterpenes like α-pinene, β-pinene and *cis*-ocimene are emitted by *Q. ilex*. However, when studying the profile of vertical wind velocity (data not shown), we estimated the air retention time in the canopy to be less than 5 min in the day hours. Such a short retention time would not allow significant ozone losses by monoterpenes. Our hypothesis is also supported by the evidence that total ozone fluxes during summer were low and comparable to winter and fall. If temperature-dependent BVOC emission promoted chemical ozone fluxes, we would have expected to observe large fluxes in summer as in previous studies (Kurpius and Goldstein, 2003; Fares et al., 2010b).

Under conditions of low turbulence, nocturnal ozone losses by reactions between ozone and monoterpenes emitted by *Q. ilex* may contribute to ozone removal as previously demonstrated (Stewart et al., 2013). This could explain an unresolved sink of about $-0.5\,\mathrm{nmol\,m^{-2}\,s^{-1}}$. We cannot exclude, however, a residual stomatal contribution to ozone deposition at night as previously shown (Grulke et al., 2004), or reaction with NO emitted from soil (De Arellano et al., 1993; Duyzer et al., 1997; Nemitz et al., 2000; Pilegaard, 2001; Kurpius and Goldstein, 2003; Farmer and Cohen, 2008). However, in the sandy forest soil in Castelporziano we do not expect nitrification and denitrification processes to be significant, leading to relevant amount of NO emission (Sutton et al., 2009).

In summary, chemical ozone sinks did not seem to play a major role at our forest ecosystem, as shown by a comparison of the three major ozone sinks with total ozone fluxes (Fig. 7). In each season, the sum of the individual ozone sinks averaged for the central hours of the day always exceeded the amount of total ozone fluxes measured at the site. In particular, during winter and summer the exceedances were 39 and 19%, respectively, while the estimate was closer to measurements in spring and fall, with exceedances of only 6 and 8%, respectively. The reason for this overestimation possibly lies in the large variance of the flux data, with standard errors of around 30% on average. Stomatal ozone fluxes reached values close to total fluxes in some cases, suggesting a possible overestimation as discussed above. In contrast to this study, Fares et al. (2012) found a consistent underestimation of total ozone fluxes in a Citrus orchard, although the ecosystem was a large source of reactive isoprenoids and a possible unaccounted sink for ozone was hypothesized.

4. Conclusions

Two years of continuous measurements of ozone fluxes in a Mediterranean forest ecosystem helped to understand and partition the most representative ozone sinks in this important forest ecosystem for each season in the year. Stomata represented the major sink, in agreement with previous studies at the same site and in other agricultural and forest ecosystems. Direct measurements of ozone deposition to soil provided basis to better define this sink at this Holm Oak forest site, while modelling the cuticular deposition allowed us to quantify the third major sink. During the winter season, the loss of ozone to stomata was almost as large as the total ozone deposition flux. For the rest of the year, however, the stomatal component explained <60% of the total ozone flux. Deposition to the forest floor made up typically 30% of total ozone loss. The cuticular sink was also estimated to be around 30%. Other loss pathways, such as by chemical reactions with BVOCs, were estimated to be negligible over the studied time period 2012–2013. Results in Castelporziano suggest that this peri-urban forest may play a role in removing ozone from the air, with a social benefit for the population near the densely inhabitated Italian coasts. Current research supported by direct measurements and smog chamber experiments is aimed at estimating the ozone budget measuring the total ozone removed by vegetation and the ozone formed by photochemical reactions driven by VOC emitted by Holm oak.

Acknowledgements

We thank the European Projects EXPLO3RVOC (FP7-PEOPLE-2012-CIG, proposal no. 321711), FO3REST (LIFE10 ENV/FR/208), ECLAIRE (FP7-ENV-2011), COST action GREENINURB (FP1204). The research was also made possible thanks to: the Scientific Commission of Castelporziano, in particular the President, Prof. Ervedo Giordano; the Multi-disciplinary Center for the Study of Coastal Mediterranean Ecosystems, in particular Ing. Aleandro Tinelli and Dr. Luca Maffei, for technical and logistic support allowing execution of these studies and publication of the data; the General Secretariat of the Presidency of Italian Republic which financed the CASTEL2 project, and the Directorate of Castelporziano Estate; the PRIN 2010/2011 TREECITY project, the team members of the biometeorology laboratory at CRA: Mr Roberto Moretti, Mr. Valerio Moretti, Mr. Tiziano Sorgi and Mr. Filippo Ilardi, for their help with setting up the experimental station; Dr Gerardo Fratini from LICOR Biogeosciences for helping to implement the ozone flux processing routines. Castelporziano is one of the Transnational Access site of the FP7 INFRA I3 project ExpeER (contract no. 262060) and financial support by the Access to Research Infrastructures activity is gratefully acknowledged.

References

Aubinet, M., Vesala, T., Papale, D., 2012. Eddy Covariance: A Practical Guide to Measurement and Data Analysis. Springer, Dordrecht, Heidelberg, London, New York, 438pp.

Baldocchi, D., 1988. A multi-layer model for estimating sulfur dioxide deposition to a deciduous oak forest canopy. Atmos. Environ. 22 (5), 869–884.

Bauer, M.R., Hultman, N.E., Panek, J.A., Goldstein, A.H., 2000. Ozone deposition to a ponderosa pine plantation in the Sierra Nevada Mountains (CA): a comparison of two different climatic years. J. Geophys. Res. 105, 123–136.

BEMA, 1997. A European commission project on biogenic emission in the Mediterranean area. Atmos. Environ. 31, 1–255.

Ciccioli, P., Brancaleoni, C., Frattoni, M., Marta, S., Brachetti, A., Vitullo, M., Tirone, G., Valentini, R., 2003. Relaxed eddy accumulation, a new technique for measuring emission and deposition fluxes of volatile organic compounds by capillary gas chromatography and mass spectrometry. J. Chromatogr. A 985, 283–296.

Davison, B., Taipale, R., Langford, B., Misztal, P., Fares, S., Matteucci, G., Loreto, F., Cape, J.N., Rinne, J., Hewitt, C.N., 2009. Concentrations and fluxes of volatile organic compounds above a Mediterranean macchia ecosystem in western Italy. Biogeosciences 6, 1655–1670.

De Arellano, J.V.G., Duynkerke, P.G., Builtjes, P.J.H., 1993. The divergence of the turbulent diffusion flux in the surface layer due to chemical reactions: the $NO–O_3–NO_2$ system. Tellus Ser. B 45, 23–33.

Detto, M., Katul, G.G., 2007. Simplified expressions for adjusting higher-order turbulent statistics obtained from open path gas analyzers. Boundary Layer Meteorol. 122 (1), 205–216.

Dorsey, J.R., Duyzer, J.H., Gallagher, M.W., Coe, H., Pilegaard, K., Weststrate, J.H., Jensen, N.O., Walton, S., 2004. Oxidized nitrogen and ozone interaction with forests. I: Experimental observations and analysis of exchange with Douglas fir. Q. J. R. Meteorolog. Soc. 130, 1941–1955.

Duyzer, J., Weststrate, H., Verhagen, H., Deinum, G., Baak, J., 1997. Measurements of dry deposition fluxes of nitrogen compounds and ozone. In: Slanina, S. (Ed.), Biosphere–Atmosphere Exchange of Pollutants and Trace Substances: Experimental and Theoretical Studies of Biogenic Emissions and Pollutant Deposition, 4. Springer, Berlin Heidelberg, pp. 244–250.

Erisman, J.W., van Pul, A., Wyers, P., 1994. Parameterization of surface resistance for the quantification of atmospheric deposition of acidifying pollutants and ozone. Atmos. Environ. 28, 2595–2607.

Escobedo, J.F., Nowak, D.J., 2009. Spatial heterogeneity and air pollution removal by an urban forest. Landscape Urban Plann. 90, 102–110.

Fares, S., Mereu, S., Scarascia Mugnozza, G., Vitale, M., Manes, F., Frattoni, M., Ciccioli, P., Gerosa, G., Loreto, F., 2009. The ACCENT-VOCBAS field campaign on biosphere–atmosphere interactions in a Mediterranean ecosystem of Castelporziano (Rome): site characteristics, climatic and meteorological conditions, and eco-physiology of vegetation. Biogeosciences 6, 1043–1058.

Fares, S., Goldstein, A., Loreto, F., 2010a. Determinants of ozone fluxes and metrics for ozone risk assessment in plants. J. Exp. Bot. 61, 629–633.

Fares, S., McKay, M., Holzinger, R., Goldstein, A.H., 2010b. Ozone fluxes in a *Pinus ponderosa* ecosystem are dominated by non-stomatal processes: evidence from long-term continuous measurements. Agric. For. Meteorol. 150, 420–431.

Fares, S., Weber, R., Park, J.-H., Gentner, D., Karlik, J., Goldstein, A.H., 2012. Ozone deposition to an orange orchard: partitioning between stomatal and non-stomatal sinks. Environ. Pollut. 169, 258–266.

Fares, S., Vargas, R., Detto, M., Goldstein, A.H., Karlik, J., Paoletti, E., Vitale, M., 2013a. Tropospheric ozone reduces carbon assimilation in trees: estimates from analysis of continuous flux measurements. Global Change Biol. 19, 2427–2443.

Fares, S., Matteucci, G., Scarascia Mugnozza, G., Morani, A., Calfapietra, C., Salvatori, E., Fusaro, L., Manes, F., Loreto, F., 2013b. Testing of models of stomatal ozone fluxes with field measurements in a mixed Mediterranean forest. Atmos. Environ. 67, 242–251.

Farmer, D.K., Cohen, R.C., 2008. Forest nitrogen oxide emissions: evidence for rapid HO_x chemistry within the canopy. Atmos. Chem. Phys. 8, 3899–3917.

Foken, T., Wichura, B., 1996. Tools for quality assessment of surface-based flux measurements. Agric. For. Meteorol. 78, 83–105.

Fowler, D., Pilegaard, K., Sutton, M.A., Ambus, P., Raivonen, M., Duyzer, J., Simpson, D., Fagerli, H., Fuzzi, S., Schjoerring, J.K., Grainer, C., Neftel, A., Isaksen, I.S.A., Laj, P., Maione, M., Monks, P.S., Burkhardt, J., Daemmgen, U., Neirynck, J., Personne, E., Wichink-Kruit, R., Butterbach-Bahl, K., Flechard, C., Tuovinen, J.P., Coyle, M., Gerosa, G., Loubet, B., Altimir, N., Gruenhage, L., Ammann, C., Cieslik, S., Paoletti, E., Mikkelsen, T.N., Ro-Poulsen, H., Cellier, P., Cape, J.N., Horvath, L., Loreto, F., Niinemets, U., Palmer, P.I., Rinne, J., Misztal, P., Nemitz, E., Nilsson, D., Pryor, S., Gallagher, M.W., Vesala, T., Skiba, U., Brueggemann, N., Zechmeister-Boltenstern, S., Williams, J., O'Dowd, C., Facchini, M.C., de Leeuw, G., Flossman, A., Chaumerliac, N., Erisman, J.W., 2009. Atmospheric composition change: ecosystems–atmosphere interactions. Atmos. Environ. 43, 5193–5267.

Gerosa, G., Finco, A., Mereu, S., Vitale, M., Manes, F., Denti, A.B., 2009. Comparison of seasonal variations of ozone exposure and fluxes in a Mediterranean Holm Oak Forest between the exceptionally dry 2003 and the following year. Environ. Pollut. 157, 1737–1744.

Groot, R.S., Wilson, A., Boumans, M.J., 2002. A typology for the classification, description and valuation of ecosystems functions, goods and services. Ecol. Econ. 41, 393–408.

Grulke, N.E., Alonso, R., Nguyen, T., Cascio, C., Dobrowolski, W., 2004. Stomata open at night in pole-sized and mature ponderosa pine: implications for O_3 exposure metrics. Tree Physiol. 24, 1001–1010.

Grulke, N.E., Paoletti, E., Heath, R.L., 2007. Comparison of calculated and measured foliar O_3 flux in crop and forest species. Environ. Pollut. 146, 640–647.

Hsieh, C., Katul, G., Chi, T., 2000. An approximate analytical model for footprint estimation of scalar fluxes in thermally stratified atmospheric flows. Adv. Water Resour. 23, 765–772.

Kalabokas, P.D., Repapis, C.C., 2004. A climatological study of rural surface ozone in central Greece. Atmos. Chem. Phys. 4, 1139–1147.

Kurpius, M.R., Goldstein, A.H., 2003. Gas-phase chemistry dominates O_3 loss to a forest, implying a source of aerosols and hydroxyl radicals to the atmosphere. Geophys. Res. Lett. 30 (7), 1371, http://dx.doi.org/10.1029/2002GL016785.

.Laisk, A., Kull, O., Moldau, H., 1989. Ozone concentration in leaf intercellular air spaces is close to zero. Plant Physiol. 90, 1163–1167.

Lamaud, E., Carrara, A., Brunet, Y., Lopez, A., Druilhet, A., 2002. Ozone fluxes above and within a pine forest canopy in dry and wet conditions. Atmos. Environ. 36, 77–88.

Launiainen, S., Katul, G.G., Gronholm, T., Vesala, T., 2013. Partitioning ozone fluxes between canopy and forest floor by measurements and a multi-layer model. Agric. For. Meteorol. 173, 85–99.

Loreto, F., Fares, S., 2013. Biogenic volatile organic compounds and their impacts on biosphere–atmosphere interactions. In: Matyssek, R., Clarke, N., Cudlin, P., Mikkelsen, T.N., Tuovinen, J.-P., Wieser, G., Paoletti, E. (Eds.), Climate Change, Air Pollution and Global Challenges: Knowledge, Understanding and Perspectives from Forest Research. Elsevier Physical Sciences Series Developments in Environmental Science. Elsevier, Amsterdam, pp. 57–75 (S. Krupa Ed.).

Manes, F., Seufert, G., Vitale, M., 1997. Ecophysiological studies of Mediterranean plant species at the Castelporziano estate. Atmos. Environ. 31, 51–60.

Manes, F., Vitale, M., Fabi, A.M., De Santis, F., Zona, D., 2007. Estimates of potential ozone stomatal uptake in mature trees of *Quercus ilex* in a Mediterranean climate. Environ. Exp. Bot. 59, 235–241.

Massman, W.J., 1998. A review of the molecular diffusivities of H_2O, CO_2,CH_4, CO, O_3, SO_2, NH_3, N_2O, NO, and NO_2 in air, O_2 and N_2 near STP. Atmos. Environ. 32, 1111–1127.

Mereu, S., Salvatori, E., Fusaro, L., Gerosa, G., Muys, B., Manes, F., 2009. A whole plant approach to evaluate the water use of mediterranean maquis species in a coastal dune ecosystem. Biogeosciences 6, 1713–1746.

Meszaros, R., Horvath, L., Weidinger, T., Neftel, A., Nemitz, E., Dammgen, U., Cellier, P., Loubet, B., 2009. Measurement and modelling ozone fluxes over a cut and fertilized grassland. Biogeosciences 6, 1987–1999.

Meyers, T.P., Baldocchi, D.D., 1993. Trace gas exchange above the floor of a deciduous forest 2. SO_2 and O_3 deposition. J. Geophys. Res.: Atmos. 98 (D7), 12631–12638, http://dx.doi.org/10.1029/93JD00720.

Millan, M.M., Mantilla, E., Salvador, R., Carratala, A., Sanz, M.J., Alonso, L., Gangoiti, G., Navazo, M., 2000. Ozone cycles in the western Mediterranean basin: interpretation of monitoring data in complex terrain. J. Appl. Meteorol. 4, 487–507.

Monks, P.S., Granier, C., Fuzzi, S., Stohl, A., Williams, M., Akimoto, H., Amman, M., Baklanov, A., Baltensperger, U., Bey, I., Blake, N., Blake, R.S., Carslaw, K., Cooper, O.R., Dentener, F., Fowler, D., Fragkou, E., Frost, G., Generoso, S., Ginoux, P., Grewe, V., Guenther, A., Hansson, H.C., Henne, S., Hjorth, J., Hofzumahaus, A., Huntrieser, H., Isaksen, I.S.A., Jenkin, M.E., Kaiser, J., Kanakidou, M., Klimont, Z., Kulmala, M., Laj, P., Lawrence, M.G., Lee, J.D., Liousse, C., Maione, M., McFiggans, G., Metzger, A., Mieville, A., Moussiopoulos, N., Orlando, J.J., O'Dowd, C., Palmer, P.I., Parrish, D.D., Petzold, A., Platt, U., Poeschl, U., Prévôt, A.S.H., Reeves, C.E., Reimann, S., Rudich, Y., Sellegri, K., Steinbrecher, R., Simpson, D., ten Brink, H., Theloke, J., Van der Werf, G.R., Vautard, R., Vestreng, V., Vlachokostas Ch VonGlasow, R., 2009. Atmospheric composition change—global and regional air quality. Atmos. Environ. 43 (33), 5264–5344.

Monteith, J.L., Unsworth, M.H., 1990. Principles of Environmental Physics. Edward Arnold, Hodder Headline PLC, London.

Muller, J.B.A., Percival, C.J., Gallagher, M.W., Fowler, D., Coyle, M., Nemitz, E., 2010. Sources of uncertainty in eddy covariance ozone flux measurements made by dry chemiluminescence fast response analysers. Atmos. Meas. Tech. 3, 163–176, http://dx.doi.org/10.5194/amt-3-163-2010.

Nemitz, E., Sutton, M.A., Wyers, G.P., Otjes, R.P., Schjørring, J.K., Gallagher, M.W., Parrington, J., Fowler, D., Choularton, T.W., 2000. Surface/atmosphere exchange and chemical interaction of gases and aerosols over oilseed rape. Agric. For. Meteorol. 105, 427–445.

Oettl, D., Uhrner, U., 2011. Development and evaluation of GRAL-C dispersion model, a hybrid Eulerian–Lagrangian approach capturing $NO–NO_2–O_3$ chemistry. Atmos. Environ. 45, 839–847.

Paoletti, E., 2006. Impact of ozone on Mediterranean forests: a review. Environ. Pollut. 144, 463–474.

Paoletti, E., Schaub, M., Matyssek, R., Wieser, G., Augustaitis, A., Bastrup-Birk, A.M., Bytnerowicz, A., Günthardt-Goerg, M.S., Müller-Starck, G., Serengil, Y., 2010. Advances of air pollution science: from forest decline to multiple-stress effects on forest ecosystem services. Environ. Pollut. 158, 1986–1989.

Papale, D., Reichstein, M., Canfora, E., Aubinet, M., Bernhofer, C., 2006. Towards a more harmonized processing of eddy covariance CO_2 fluxes: algorithms and uncertainty estimation. Biogeosciences 3, 571–583.

Pellegrini, E., Lorenzini, G., Nali, C., 2007. The 2003 European heat wave: which role for ozone? Some data from Tuscany, Central Italy. Water Air Soil Pollut. 181, 401–408.

Pilegaard, K., 2001. Air–soil exchange of NO, NO_2 and O_3 in forests. Water Air Soil Pollut. 1, 79–88.

Pleijel, H., Danielsson, H., Ojanper, K., De Temmerman, L., Hogy, P., Badiani, M., Karlsson, P.E., 2004. Relationships between ozone exposure and yield loss in European wheat and potato—a comparison of concentration- and flux-based exposure indices. Atmos. Environ. 38, 2259–2269.

Rissmann, J., Tetzlaff, G., 1994. Application of a spectral correction method for measurements of covariances with fast-response sensors in the atmospheric boundary layer up to aheight of 130 m and testing of the corrections. Boundary Layer Meteorol. 70 (3), 293–305.

Seok, B., Helmig, D., Ganzeveld, L., Williams, M.W., Vogel, C.S., 2013. Dynamics of nitrogen oxides and ozone above and within a mixed hardwood forest in northern Michigan. Atmos. Chem. Phys. 13, 7301–7320.

Serengil, Y., Augustaitis, A., Bytnerowicz, A., Grulke, N., Kozovitz, A.R., Matyssek, R., Müller-Starck, G., Schaub, M., Wieser, G., Coskun, A.A., Paoletti, E., 2011. Adaptation of forest ecosystems to air pollution and climate change: a global assessment on research priorities. iForest 4, 44–48.

Smeets, C.J.P.P., Holzinger, R., Vigano, I., Goldstein, A.H., Röckmann, T., 2009. Eddy covariance methane measurements at a Ponderosa pine plantation in California. Atmos. Chem. Phys. 9, 8365–8375.

Stewart, D.J., Almabrok, S.H., Lockhart, J.P., Mohamed, O.M., Nutt, D.R., Pfrang, C., Marston, G., 2013. The kinetics of the gas-phase reactions of selected monoterpenes and cyclo-alkenes with ozone and the NO_3 radical. Atmos. Environ. 70, 227–235.

Sutton, M.A., Nemitz, E., Theobald, M.R., Milford, C., Dorsey, J.R., Gallagher, M.W., Hensen, A., Jongejan, P.A.C., Erisman, J.W., Mattsson, M., Schjoerring, J.K., Cellier, P., Loubet, B., Roche, R., Neftel, A., Hermann, B., Jones, S.K., Lehman, B.E., Horvath, L., Weidinger, T., Rajkai, K., Burkhardt, J., Löpmeier, F.J., Daemmgen, U., 2009. Dynamics of ammonia exchange with cut grassland: strategy and implementation of the GRAMINAE Integrated Experiment. Biogeosciences 6, 309–331.

Turnipseed, A.A., Burns, S.P., Moore, D.J.P., Hu, J., Guenther, A.B., Monson, R.K., 2009. Controls over ozone deposition to a high elevation subalpine forest. Agric. For. Meteorol. 149, 1447–1459.

Tuzet, A., Perrier, A., Loubet, B., Cellier, P., 2011. Modelling ozone deposition fluxes: the relative roles of deposition and detoxification processes. Agric. For. Meteorol. 151 (4), 480–492.

Vargas, R., Sonnentag, O., Abramowitz, G., Carrara, A., Chen, J.M., Ciais, P., Correia, A., Keenan, T.F., Kobayashi, H., Ourcival, J.-M., Papale, D., Pearson, D., Pereira, J.S., Piao, S., Rambal, S., Baldocchi, D.D., 2013. Drought influences the accuracy of simulated ecosystem fluxes: a model-data meta-analysis for Mediterranean oak woodlands. Ecosystems 16, 749–764.

Velchev, K., Cavalli, F., Hjorth, J., Marmer, E., Vignati, E., Dentener, F., Raes, F., 2011. Ozone over the Western Mediterranean Sea—results from two years of ship-borne measurements. Atmos. Chem. Phys. 11, 675–688.

Vingarzan, R., 2004. A review of surface ozone background levels and trends. Atmos. Environ. 38, 3431–3442.

Webb, E.K., Pearman, G.I., Leuning, R., 1980. Correction of flux measurements for density effects due to heat and water vapour transfer. Q. J. R. Meteorolog. Soc. 106, 85–100.

Wilczak, J.M., Oncley, S.P., Stage, S.A., 2001. Sonic anemometer tilt correction algorithms. Boundary Layer Meteorol. 99, 127–150.

Wilson, K.B., Hanson, P.J., Mulholland, P.J., Baldocchi, D.D., Wullschleger, S.D., 2001. A comparison of methods for determining forest evapotranspiration and its components: sap-flow, soil water budget, eddy covariance and catchment water balance. Agric. For. Meteorol. 106, 153–168.
Wilson, K.B., Meyers, T.P., 2001. The spatial variability of energy and carbon dioxide fluxes at the floor of a deciduous forest. Boundary Layer Meteorol. 98, 443–473.
Wittig, V.E., Ainsworth, E.A., Naidu, S.L., Karnosky, D.F., Long, S.P., 2009. Quantifying the impact of current and future tropospheric ozone on tree biomass, growth, physiology and biochemistry: a quantitative meta-analysis. Global Change Biol. 15, 396–424.
Zhang, L., Brook, J.R., Vet, R., 2002. On ozone dry deposition with emphasis on non-stomatal uptake and wet canopies. Atmos. Environ. 36, 4787–4799.